International Orthopaedics (2019) 43:1521–1528
https://doi.org/10.1007/s00264-018-4053-1

ORIGINAL PAPER

Morphometry evaluations of cervical osseous endplates based on three dimensional reconstructions

Hang Feng[1] · Haoxi Li[1] · Zhaoyu Ba[1] · Zhaoxiong Chen[1] · Xinhua Li[1] · Desheng Wu[1]

Received: 22 January 2018 / Accepted: 6 July 2018 / Published online: 9 August 2018

Abstract

Purpose Accurate and comprehensive data on cervical endplates is essential for developing and improving cervical devices. However, current literature on vertebral disc geometry is scarce or not suitable. The aim of this study was to obtain quantitative parameters of cervical endplates and provide morphometric references for designing cervical devices.

Methods In this study, 19 human cervical spine cadaveric specimens were considered. Employing a reverse engineering system, the surface information of each endplate was recorded in digital cloud and then 3D reconstructed. A measurement protocol that included three sagittal and three frontal surface curves was developed. The information of surface curves and endplate concavity were obtained and analyzed. The parametric equations of endplate surfaces were deduced based on coordinates of landmarks, and the reliability was verified.

Results The cervical endplate surface had a trend that to be transversely elongated gradually. The concavity depths of inferior endplates (1.88 to 2.13 mm) were significantly larger than those of superior endplates (0.62 to 0.84 mm). The most-concave points in inferior endplates were concentrated in the central portion, while always located in post-median region in superior endplates.

Conclusion These results will give appropriate guidelines to design cervical prostheses without sacrificing valuable bone stock. The parametric equations applied for generating surface profile of cervical endplates may provide great convenience for subsequent studies.

Keywords Morphology · Cervical vertebra endplates · Cervical prostheses · Anatomy

Introduction

With the increasing incidence of cervical spondylosis, anterior cervical discectomy and fusion and cervical disc replacements as surgical interventions have gained more and more common. However, there is a large disparity that the anatomic dimensions of cervical endplates are generally larger than the frequently implanted cervical devices [1–3]. Moreover, the surface of almost all prostheses used now is designed relatively flat [4, 5], while the osseous endplate geometry is concave [6]. To adapt the geometry of the disc space to the shape of the cage, the endplates have to be modified with partial or even complete removal, which destroys the structural integrity and reduces both the failure load and stiffness of the endplates [7]. A number of studies have confirmed that too small or incongruent contact area can facilitate implant subsidence as a result of extremely concentrated stress [8, 9].

Therefore, an ideal device should mirror the three dimensions of cervical endplate morphology. And accurately and comprehensively quantitative data of vertebral endplate is prerequisite for developing and improving cervical devices. However, previous studies, mainly focusing on anteroposterior diameter and width, or concavity in midsagittal plane, could not adequately describe the endplate morphology [5, 6, 10–12]. In addition, the accuracy and reliability of existing geometric data may be problematic due to the lack of a standardized measurement protocol and lower precision measuring instruments [7, 13]. Some studies have reported

Electronic supplementary material The online version of this article (https://doi.org/10.1007/s00264-018-4053-1) contains supplementary material, which is available to authorized users.

✉ Desheng Wu
spinewudesheng@126.com

[1] Department of Spinal Surgery, Shanghai East Hospital, Tongji University School of Medicine, 150 JiMo Road, Shanghai 200120, China

there is significant magnification for linear measurements in digital radiography and significant overstatement for endplate thickness measurement employing CT [14–16].

In recent years, reverse engineering has been increasingly applied to medicine field, which can digitize existing physical parts into computerized solid models [17]. The aims of this study were to conduct a cadaveric study to obtain quantitative parameters of cervical endplates employing reverse engineering technique, and to provide morphology references for the designing of cervical devices.

Materials and methods

Samples and reverse engineering system

A total of 138 endplates (68 inferior and 70 superior) from 19 cervical spines (16 males and 3 females, average age 53 years; age range 38–64 years) were used in the current study. Exclusion criteria included significant osteophyte formation, obvious degeneration, vertebral fractures, and poorly scanned images in image collection process. The study was approved by the health research ethics board of the author's institute.

The reverse engineering system employed in the present study includes two subsystems: the instrumentation system and the software system. The instrumentation system is a non-contact optical 3D range flatbed scanner (XTOM-micro I, Xi'an XinTuo 3D Optical Measurement Technology Co. Ltd., Xi'an, Shaanxi, China), which can efficiently capture the surface morphology of a targeted object and convert the corresponding information into digital point cloud. The precision of this system is 0.02 mm, pixel is 1628 × 1236, and the input time is three seconds. In the software system, the point cloud is further processed (Geomagic Studio, version 12; Geomagic Inc., Morrisville, NC) and created a 3D surface model (Catia, version V5R20; Dassault System, Paris, France).

Measurement of the endplate morphology

With the help of the instrumentation system, the surface information of each endplate was recorded. And the endplate was extracted and 3D reconstructed in the software system.

Before measurements were conducted, a 3D coordinate system was defined to transform the digitized points into local coordinate system. Initially, an axial reference plane was defined using three points from the epiphyseal rim: one is the anterior median point of epiphyseal rim, and the rest two were the left and right endpoints of endplate trailing edge. A reference line was determined by the two endpoints, and the origin of the coordinate system coincided with the centroid of the reference plane. The line perpendicular to the reference line formed the *z*-axis, and the line parallel to the reference line formed the *x*-axis, and the *y*-axis was perpendicular to the reference plane. The mid-sagittal diameter and the mid-frontal diameter were divided into four equal parts. Then, going through every equidistant point, six surface curves were symmetrically chosen on each endplate that three curves in the sagittal plane and the other three in the frontal plane. Then, 11 equal points were selected in each curve for subsequent measurements (Fig. 1).

The linear parameters of each curve were the distance between the two endpoints. The endplate concavity depth (ECD) was the perpendicular distance from the most concave point to the axial reference plane. Similarly, the mid-sagittal plane

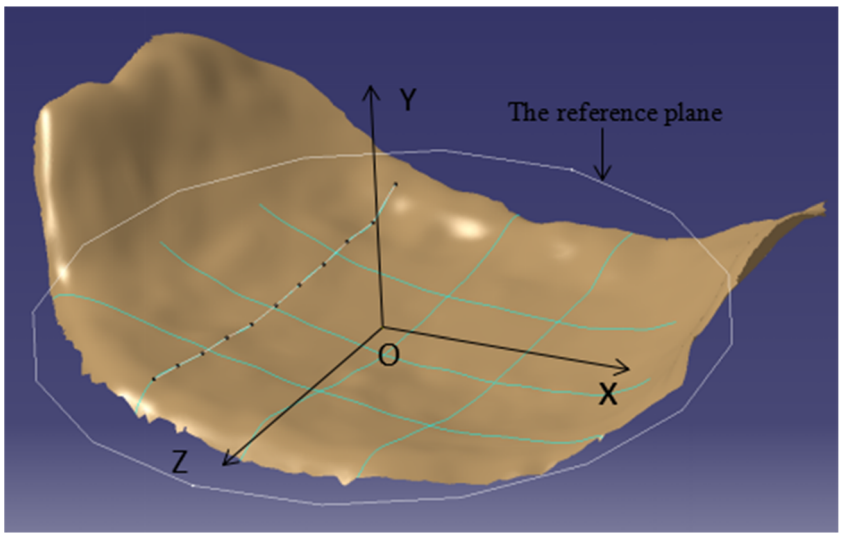

Fig. 1 Definition of the cervical vertebra endplate coordinate system and the schematic of the measurement protocol

Table 1 Reliability of measurements

Measurements		Intra-test reliability	Measurements		RE vs caliper
APD	First remeasurement	15.76 ± 1.3	APD	RE	16.47 ± 1.31
	Remeasurement	15.86 ± 1.61		Caliper	16.26 ± 1.27
ICC		0.85	Cronbach alpha		0.99
CMD	First remeasurement	19.71 ± 2.47	CMD	RE	20.7 ± 3.05
	Remeasurement	19.41 ± 2.43		Caliper	20.45 ± 3.21
ICC		0.96	Cronbach alpha		0.99

Data were mean ± standard deviation

ICC, intra-class correlation coefficient; *APD*, anteroposterior diameter; *CMD*, center mediolateral diameter; *RE*, the reverse engineering system

endplate concavity depth (SCD) and the mid-frontal plane endplate concavity depth (FCD) could also be obtained. In addition, the location of the projective point that the most concave point casted in the axial reference plane was also recorded. For the sake of obtaining data of endplate surface conveniently and efficiently in subsequent studies, parametric equations of endplate surface were deduced based on coordinates of 66 points using the polynomial fitting method in MATLAB (version R2014a; The MathWorks Inc., Natick, USA).

Verification: repeatability of measurements

For intra-test reliability, 16 samples were randomly measured two rounds at a two week interval and were assessed using intra-class correlation coefficient (ICC). To verify the accuracy of the measurements taken by the reverse engineering system, 20 samples were measured using a digital caliper (Hengliang tools Co. Ltd., Shanghai, China, Precision ± 0.01 mm) and were evaluated using Cronbach alpha. The values measured for reliability tests were the anteroposterior diameter and the mediolateral diameter.

Statistical analysis

The SPSS software (version 18.0, SPSS Inc., Chicago, IL, USA) was employed for statistical analyses. *T* tests were applied for the comparison of parameters between two groups. Multiple comparisons were compared using analysis of variance (ANOVA). The statistical significance level was set at $p < 0.05$.

Results

Reliability of the measurements

As shown in Table 1, these values showed great agreement, as the value of ICC greater than 0.75 indicates good reliability

Table 2 The length of six fitting curves on the endplate (mm)

Endplate level		Sagittal plane curves			Frontal plane curves		
	N	SLL	SML	SRL	FAL	FML	FPL
C3 inf	19	13.37 ± 1.36	13.71 ± 1.81	13.55 ± 1.65	12.77 ± 1.07	13.84 ± 1.47	12.87 ± 1.69
C4 sup	16	11.65 ± 1.48	12.25 ± 1.75	11.66 ± 1.7	13.53 ± 1.98	14.56 ± 1.42	13.22 ± 1.57
C4 inf	15	13.69 ± 1.74	14.07 ± 1.67	13.75 ± 1.66	12.97 ± 1.22	14.54 ± 1.28	13.9 ± 1.83
C5 sup	19	11.44 ± 1.32	12.08 ± 1.38	11.44 ± 1.28	14.55 ± 1.44	15.23 ± 1.35	13.96 ± 1.83
C5 inf	17	13.4 ± 1.66	13.91 ± 1.59	13.44 ± 1.52	15.22 ± 1.97	16.33 ± 1.62	15.21 ± 2.33
C6 sup	18	12.23 ± 1.21	12.98 ± 1.36	12.52 ± 1.32	15.91 ± 1.93	16.7 ± 1.9	15.23 ± 1.58
C6 inf	17	13.94 ± 1.71	14.15 ± 1.68	13.95 ± 1.76	17.94 ± 2.29	19.08 ± 1.94	17.43 ± 1.89
C7 sup	17	12.9 ± 1.38	13.37 ± 1.33	13.09 ± 1.42	16.62 ± 2.32	19.61 ± 2.16	17 ± 1.89

SLL, length of sagittal left curve; *SMC*, length of sagittal middle curve; *SRC*, length of sagittal right curve; *FAL*, length of frontal anterior curve; *FML*, length of frontal middle curve; *FPL*, length of frontal posterior curve

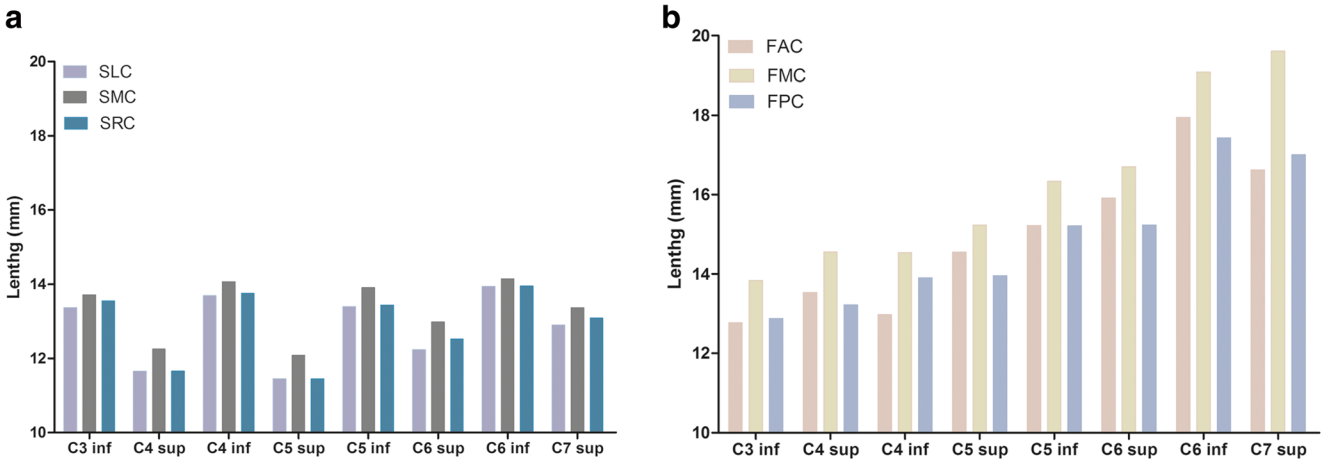

Fig. 2 The lengths and trends of the curves on the inferior (**a**) and superior (**b**) endplates

[18] and alpha values of 0.7–0.8 are regarded as satisfactory [19].

Measurements of vertebral endplate geometry

The lengths of the curves were listed in Table 2 and their trends were presented in Fig. 2. Overall, the lengths of the sagittal curves were relatively constant, while the frontal curves showed a significant increase and greater than the corresponding sagittal curves especially from C5 to C7. That is to say the cervical endplate surface had a trend that to be transversely elongated gradually. Within each endplate, the lengths of the middle curves both on the sagittal and coronal planes were greater than curves on their both sides, and there was no statistical difference when compared the two side curves. When compared sagittal curves between inferior and superior endplates adjacent to the same cervical disc, the former were always larger than the latter. However, with respect to the frontal planes, the inferior curves were generally slightly smaller.

Inferior ECD ranged from 1.88 to 2.13 mm, while superior ECD ranged from 0.62 to 0.84 mm (Table 3). Within each endplate, the ECD was always greater than SCD and FCD ($p < 0.001$). Most-concave points on inferior endplates were concentrated in the central portion; while the distribution of superior endplate most-concave points was relatively dispersed, even so, the majority of them located in post-median region (Fig. 3).

Mathematical modeling for cervical vertebral endplate

The fit order of the equation was determined before fitting function. In order to obtain higher precision, the present study sets the sums of squared error smaller than 0.01, and it was concluded that using the four-order function could achieve satisfaction.

The parametric equation to represent the morphology of endplate surface was:

$$F(x,z) = p00 + p10^{*}x + p01^{*}z + p20^{*}x^{2} + p11^{*}x^{*}z + p02^{*}z^{2} + p30^{*}x^{3} + p21^{*}x^{2}{*}z + p12^{*}x^{*}z^{2} + p03^{*}z^{3} + p40^{*}x^{4} + p31^{*}x^{3}{*}z + p22^{*}x^{2}{*}z^{2} + p13^{*}x^{*}z^{3} + p04^{*}z^{4}$$

The P_X were the parameters, and their exact values were showed in Appendix Table 4. The validity of the geometric model representing the endplate morphology was evaluated by comparing coordinate value of 15 randomly selected points with their corresponding value auto-generated from parametric equations. The statistical results revealed it was accurate and reproducible to represent endplate surface ($R = 0.98$, $p <$

Table 3 The whole endplate and mid-sagittal and mid-frontal plane endplate concavity depth

Endplate level	ECD	SCD	FCD
C3 inf	2.13 ± 0.57	2.09 ± 0.59	2.06 ± 0.55
C4 sup	0.64 ± 0.2	0.61 ± 0.21	0.48 ± 0.28
C4 inf	2.13 ± 0.53	2.08 ± 0.57	1.95 ± 0.69
C5 sup	0.62 ± 0.23	0.58 ± 0.23	0.37 ± 0.22
C5 inf	2.01 ± 0.45	1.96 ± 0.45	1.99 ± 0.44
C6 sup	0.68 ± 0.31	0.66 ± 0.33	0.5 ± 0.32
C6 inf	1.88 ± 0.37	1.86 ± 0.37	1.83 ± 0.38
C7 sup	0.84 ± 0.35	0.77 ± 0.37	0.66 ± 0.39

ECD, the whole endplate concavity depth; *SCD*, the mid-sagittal plane endplate concavity depth; *FCD*, the mid-frontal plane endplate concavity depth

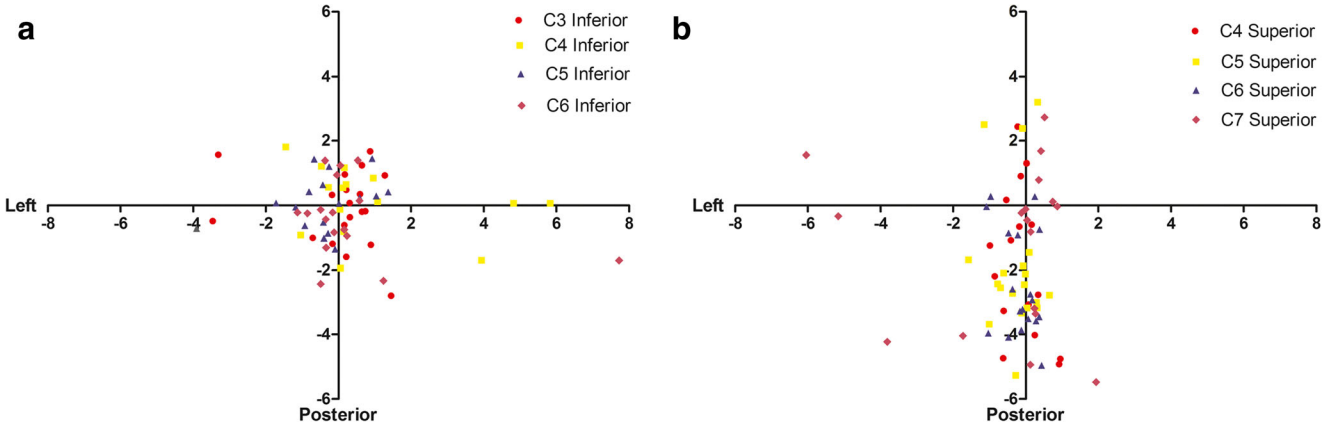

Fig. 3 The distribution of the location of the most-concave point in the axial reference plane. **a**, **b** The distribution on the upper and lower endplates, respectively

0.001). Figure 4 was a personalized 3D representation of cervical endplate (C5 inferior), and it could be observed that the 3D reconstruction image matched well with the selected landmarks.

Discussion

With surgical techniques widely used for treating symptomatic cervical degenerative disc disease and longer follow-up, more and more researchers have paid attention to the increasing post-operative complications related with morphologic mismatch between anatomic geometry of cervical endplates and prostheses.

Subsidence is a commonly known complication, which may lead to gradual loss of anterior column and foraminal height, kyphosis, and recurrence of radiculopathy. One of main causes is inadequate load distribution associated with failure of device design [8]. It has been realized that undersized prostheses may contribute to subsidence, as they create the limited contact area leading to extremely concentrated stress at the prosthesis-endplate interface, and lack support from peripheral marginal zones [8, 20]. Just as a striking example described, "If we observe two people standing on soft snow, one wearing a pair of boots and the other wearing skis, we can easily notice that the person wearing boots stands deeper in the snow than the skier" [21]. A retrospective analysis performed by Mende et al. [20] found a significantly higher subsidence rate for patients with cages that were small

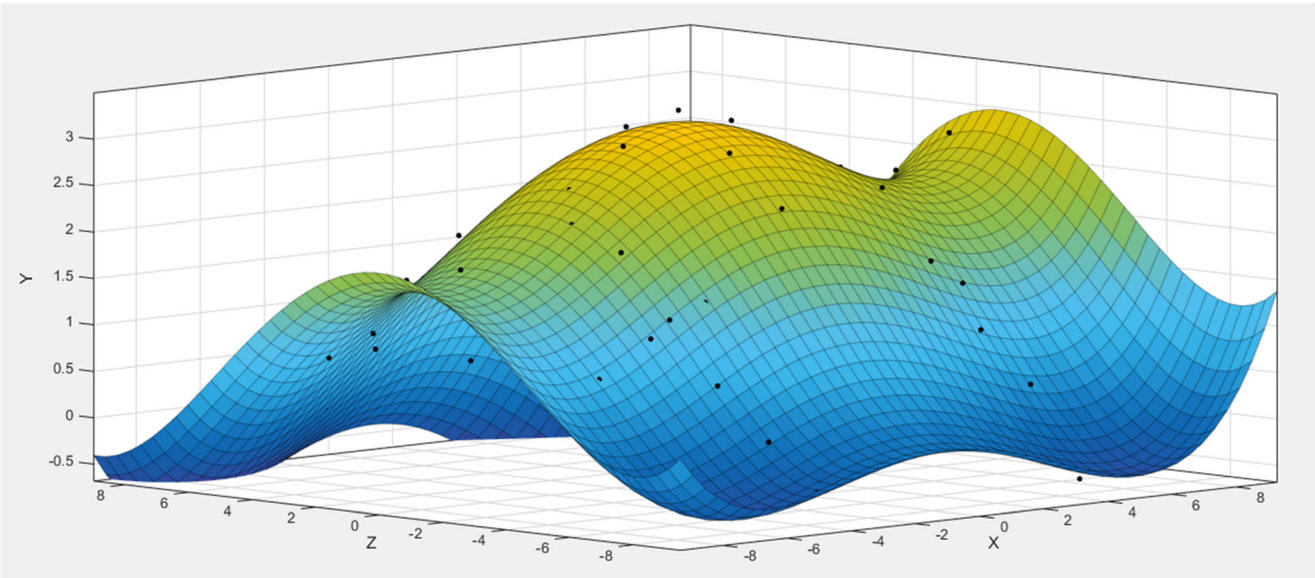

Fig. 4 The endplate (C5 inferior) was reconstructed in the MATALB software, according to its parametric equation. Those scattered points represented the selected landmarks on the original 3D reconstruction image

in relation to their anatomy with a cage to endplate surface ratio below 65%.

Not only prosthesis shape but also geometric profile affects the compressive strength at the prosthesis-endplate interface [9]. The contour of vertebral endplates has an arched shape with inner region concave. However, the prosthesis in clinical application is designed relatively flat or slightly convex compare to the bony endplate. To achieve a closer fit, partial or even complete of endplates has to be removed to accommodate the geometry of existing prostheses. Moreover, in order to obtain primary fixation, some accessories are designed, such as teethlike ridges, fin, and keel. However, those prosthetic designs may be highly destructive if the revision requires chiseling and unnecessary sacrifice of bone around those accessories [21]. These grinding operations compromise the integrity and strength of the endplate and reduce both the failure load and stiffness [22, 23]. Cheng et al. [24] reported that there was a significant loss of endplate integrity when 1 mm (44% loss) or 2 mm of endplate (52% loss) was removed. Recently, a biomechanical cadaveric study was conducted to evaluate pullout strength of screws used in integrated fixation cages with different endplate preparations. The results revealed that endplate scraping endplate thickness by 20% on average resulted in a decrease in fixation strength compared with the unscraped endplates [25]. Besides, some studies on cervical disc replacements have reported that the inappropriate match may cause abnormal cervical alignment and kinematics and even increase stress of the facet joint and adjacent segment [26, 27]. Moreover, the mismatch prosthesis is supposed to be related to the occurrence of heterotrophic ossification [28].

Therefore, the prostheses should have footprints as large as possible to distribute forces evenly and obtain as much support as possible from periphery, and complement well to the profile of osseous endplates to leave the endplates as intact as possible. Accurate and detailed information of vertebral endplates is important and necessary to design appropriate cervical devices. In the present study, the quantitative description of the 3D morphology of cervical vertebral endplates was conducted employing the reverse engineering system. In the measurement protocol, the linear parameter was the distance from the epiphyseal ring to epiphyseal ring, which we believed would provide more valuable reference for designing prostheses large enough to obtain support from the strong peripheral part. According to our investigation, we found that the trend that the cervical endplate cross sections to be transversely elongated gradually, which revealed the morphologic variation among vertebral segments. And there were marked morphologic asymmetries between adjacent superior and inferior endplates in 3D morphology: The lengths of sagittal curves on inferior endplates were always larger than their counterparts on superior endplates, while the frontal curves on inferior endplates were generally slightly smaller; all the inferior endplates were more concave than the corresponding superior endplates; most of most-concave points on superior endplates located in post-median region, while in terms of inferior endplates, they concentrated in central portion. To design appropriate cervical devices and develop optimal surgical plans, we suggest that these endplate morphological characteristics mentioned above should be taken into consideration. For instance, some recent studies suggest that relative anterior placement of the cage within the disc space can optimize the lordosis gain [20, 29]. However, when the prostheses and osseous endplates match ill and the fixation is insufficient, the prostheses with their maximum height at the anterior aspect may migrate to the most concave part which always locates in post-median or central region. Langrana et al. [17] conducted a finite element analysis to investigate the endplate curvature effects. The results revealed that the stress distribution was affected as the location of the maximum curvature was shift, and when the endplate curvature shifted posteriorly by nearly 50% from the center, the solid model had minimum stress value. Besides, it has been demonstrated that the posterior and lateral regions of the cervical endplate are thicker and stronger than the anterior and middle regions [7, 30]. Those discrepancies reinforce the necessity to design anatomic prostheses and perform rigorous biomechanical tests to verify their effectiveness.

The present study developed a mathematical modeling representing cervical osseous endplates and developed an algorithm capable of describing their morphological characteristics conveniently and efficiently. The reliability tests indicated that the 3D model could make a realistic representation of endplate surface, and the parametric equations had good reliability and reproducibility to quantify endplate morphology. These parametric equations can be extrapolated to get valuable information such as volume, mean depth, and depth variations and may be used to evaluate vertebral body fractures.

Conclusions

The reverse engineering methodology can effectively and accurately determine the size and profile of the vertebral endplate. The results of this present study will give appropriate guidelines to design cervical prostheses without sacrificing valuable bone stock. The parametric equations applied for generating surface profile of cervical endplates may provide great convenience for subsequent research.

Compliance with ethical standards

Conflict of interest The authors declare that they have no conflicts of interest.

Appendix

Table 4 The parameters parametric equation to represent the morphology of endplate surface

Parameters	C3 inf	C4 sup	C4 inf	C5 sup	C5 inf	C6 sup	C6 inf	C7 sup
p00	1.989	0.4187	2.004	0.3383	1.913	0.4276	1.779	0.5674
p10	0.002214	-0.004348	0.005419	-0.02082	-0.01108	0.0012	-0.004329	-0.005244
p01	0.03561	-0.08683	-0.05366	-0.08263	-0.02572	-0.09797	-0.04069	-0.06418
p20	0.01286	-0.02523	-0.01455	-0.02991	-0.0253	-0.02639	-0.01747	-0.008776
p11	0.0009194	0.000707	-0.0009397	0.0001792	-0.0002119	-0.001242	0.001172	0.0002116
p02	0.05289	-0.01514	-0.05253	-0.01196	-0.04179	-0.01421	-0.03955	-0.01336
p30	0*	-0.0001004	0.0001289	0.0002435	0.0001704	0*	0*	0*
p21	0.001071	0.002994	-0.001191	0.003626	-0.002101	0.003064	-0.001949	0.001942
p12	0*	0.0004835	-0.0004059	0.0003333	0.0001412	0*	-0.0001056	0*
p03	0.0006198	0.002039	0.0008887	0.002055	0.0004556	0.002078	0.000767	0.001152
p40	0.000204	0*	0.0002022	0*	0.0002416	0*	0*	0*
p31	0*	0*	0*	0*	0*	0*	0*	0*
p22	0.0001671	0.0001311	0*	0.0001487	0.0001473	0.0001721	0.0003209	0*
p13	0*	0*	0*	0*	0*	0*	0*	0*
p04	0.0002251	0.0001326	0.0002435	0*	0*	0*	0*	0*

Note: the value was too small and almost equal to 0

References

1. Dong L, Tan MS, Yan QH, Yi P, Yang F, Tang XS, Hao QY (2015) Footprint mismatch of cervical disc prostheses with Chinese cervical anatomic dimensions. Chin Med J 128(2):197–202. https://doi.org/10.4103/0366-6999.149200
2. Gstoettner M, Heider D, Liebensteiner M, Bach CM (2008) Footprint mismatch in lumbar total disc arthroplasty. Eur Spine J 17(11):1470–1475. https://doi.org/10.1007/s00586-008-0780-0
3. Thaler M, Hartmann S, Gstottner M, Lechner R, Gabl M, Bach C (2013) Footprint mismatch in total cervical disc arthroplasty. Eur Spine J 22(4):759–765. https://doi.org/10.1007/s00586-012-2594-3
4. de Beer N, Scheffer C (2012) Reducing subsidence risk by using rapid manufactured patient-specific intervertebral disc implants. Spine J 12(11):1060–1066. https://doi.org/10.1016/j.spinee.2012.10.003
5. Zhu YH, Cheng KL, Zhong Z, Li YQ, Zhu QS (2016) Morphologic evaluation of Chinese cervical endplate and uncinate process by three-dimensional computed tomography reconstructions for helping design cervical disc prosthesis. J Chin Med Assoc 79(9):500–506. https://doi.org/10.1016/j.jcma.2016.04.003
6. Chen H, Zhong J, Tan J, Wu D, Jiang D (2013) Sagittal geometry of the middle and lower cervical endplates. Europ Spine J 22(7):1570–1575. https://doi.org/10.1007/s00586-013-2791-8
7. Pitzen T, Schmitz B, Georg T, Barbier D, Beuter T, Steudel WI, Reith W (2004) Variation of endplate thickness in the cervical spine. Eur Spine J 13(3):235–240. https://doi.org/10.1007/s00586-003-0648-2
8. Lin CY, Kang H, Rouleau JP, Hollister SJ, Marca FL (2009) Stress analysis of the interface between cervical vertebrae end plates and the Bryan, Prestige LP, and ProDisc-C cervical disc prostheses: an in vivo image-based finite element study. Spine 34(15):1554–1560. https://doi.org/10.1097/BRS.0b013e3181aa643b
9. Steffen T, Tsantrizos A, Aebi M (2000) Effect of implant design and endplate preparation on the compressive strength of interbody fusion constructs. Spine 25(9):1077–1084
10. Kim MK, Kwak DS, Park CK, Park SH, Oh SM, Lee SW, Han SH (2007) Quantitative anatomy of the endplate of the middle and lower cervical vertebrae in Koreans. Spine 32(14):E376–E381. https://doi.org/10.1097/BRS.0b013e318067e384
11. Panjabi MM, Duranceau J, Goel V, Oxland T, Takata K (1991) Cervical human vertebrae. Quantitative three-dimensional anatomy of the middle and lower regions. Spine 16(8):861–869
12. Tan SH, Teo EC, Chua HC (2004) Quantitative three-dimensional anatomy of cervical, thoracic and lumbar vertebrae of Chinese Singaporeans. Eur Spine J 13(2):137–146. https://doi.org/10.1007/s00586-003-0586-z
13. Tang R, Gungor C, Sesek RF, Foreman KB, Gallagher S, Davis GA (2016) Morphometry of the lower lumbar intervertebral discs and endplates: comparative analyses of new MRI data with previous findings. Eur Spine J 25(12):4116–4131. https://doi.org/10.1007/s00586-016-4405-8
14. Panjabi MM, Chen NC, Shin EK, Wang JL (2001) The cortical shell architecture of human cervical vertebral bodies. Spine 26(22):2478–2484
15. Ravi B, Rampersaud R (2008) Clinical magnification error in lateral spinal digital radiographs. Spine 33(10):E311–E316. https://doi.org/10.1097/BRS.0b013e31816f6c3f
16. Silva MJ, Wang C, Keaveny TM, Hayes WC (1994) Direct and computed tomography thickness measurements of the human, lumbar vertebral shell and endplate. Bone 15(4):409–414
17. Langrana NA, Kale SP, Edwards WT, Lee CK, Kopacz KJ (2006) Measurement and analyses of the effects of adjacent end plate curvatures on vertebral stresses. Spine J 6(3):267–278. https://doi.org/10.1016/j.spinee.2005.09.008

18. Shrout PE, Fleiss JL (1979) Intraclass correlations: uses in assessing rater reliability. Psychol Bull 86(2):420–428
19. Bland JM, Altman DG (1997) Cronbach's alpha. BMJ (Clinical research ed) 314(7080):572
20. Mende KC, Eicker SO, Weber F (2017) Cage deviation in the subaxial cervical spine in relation to implant position in the sagittal plane. Neurosurg Rev. https://doi.org/10.1007/s10143-017-0850-z
21. Link HD, McAfee PC, Pimenta L (2004) Choosing a cervical disc replacement. Spine J 4(6 Suppl):294s–302s. https://doi.org/10.1016/j.spinee.2004.07.022
22. Auerbach JD, Ballester CM, Hammond F, Carine ET, Balderston RA, Elliott DM (2010) The effect of implant size and device keel on vertebral compression properties in lumbar total disc replacement. Spine J 10(4):333–340. https://doi.org/10.1016/j.spinee.2010.01.008
23. Truumees E, Demetropoulos CK, Yang KH, Herkowitz HN (2003) Failure of human cervical endplates: a cadaveric experimental model. Spine 28(19):2204–2208. https://doi.org/10.1097/01.brs.0000084881.11695.50
24. Cheng CC, Ordway NR, Zhang X, Lu YM, Fang H, Fayyazi AH (2007) Loss of cervical endplate integrity following minimal surface preparation. Spine 32(17):1852–1855. https://doi.org/10.1097/BRS.0b013e31811ece5a
25. Nagaraja S, Palepu V, Peck JH, Helgeson MD (2015) Impact of screw location and endplate preparation on pullout strength for anterior plates and integrated fixation cages. Spine J 15(11):2425–2432. https://doi.org/10.1016/j.spinee.2015.07.454
26. Dmitriev AE, Cunningham BW, Hu N, Sell G, Vigna F, McAfee PC (2005) Adjacent level intradiscal pressure and segmental kinematics following a cervical total disc arthroplasty: an in vitro human cadaveric model. Spine 30(10):1165–1172
27. Rousseau MA, Bradford DS, Hadi TM, Pedersen KL, Lotz JC (2006) The instant axis of rotation influences facet forces at L5/S1 during flexion/extension and lateral bending. Eur Spine J 15(3):299–307. https://doi.org/10.1007/s00586-005-0935-1
28. Cao JM, Zhang YZ, Shen Y, Xu JX, Ding WY, Yang DL, Zhang D (2011) Clinical and radiological outcomes of modified techniques in Bryan cervical disc arthroplasty. J Clin Neurosci 18(10):1308–1312. https://doi.org/10.1016/j.jocn.2011.01.034
29. Landham PR, Don AS, Robertson PA (2017) Do position and size matter? An analysis of cage and placement variables for optimum lordosis in PLIF reconstruction. Eur Spine J 26(11):2843–2850. https://doi.org/10.1007/s00586-017-5170-z
30. Muller-Gerbl M, Weisser S, Linsenmeier U (2008) The distribution of mineral density in the cervical vertebral endplates. Eur Spine J 17(3):432–438. https://doi.org/10.1007/s00586-008-0601-5